



SUCCESSSES AND CHALLENGES OF SYNCHROTRON X-RAY NANO-TOMOGRAPHY FOR THE CHARACTERIZATION OF SOLID OXIDE CELLS MATERIALS

Workshop on Coherence at ESRF-EBS | 12-09-2019

M. Hubert¹, F. Monaco¹, J. C. da Silva², F. Lefebvre-Joud¹, P. Cloetens², J. Laurencin¹

¹Univ. Grenoble Alpes – CEA/LITEN, 38054, Grenoble, France,

² European Synchrotron Radiation Facility (ESRF), 38000, Grenoble, France

ACKNOWLEDGMENTS

A fruitful collaboration between CEA-LITEN
and ESRF-Nano-Imaging beamline

G. Audoit

F. Lefebvre-Joud

S. Bohic

P. Bleuet

J.C. Da Silva

L. Andre

Jérôme LAURENCIN
CEA Grenoble LITEN

Peter CLOETENS
ESRF - ID16A



R. Quey

F. Monaco

G. Delette

A. Pacureanu



M. Salome

E. Lay-Grindler

H. Moussaoui

Y. Yang

H. Suhonen

F. Usseglio-Viretta

J. Villanova

CONTEXT

High temperature Solid Oxide Cell (SOC)

😊 Efficient energy conversion system

☹️ Microstructural evolution

😊 High flexibility: SOFC / SOEC modes

☹️ Electrode Poisoning

😊 No expensive catalyst

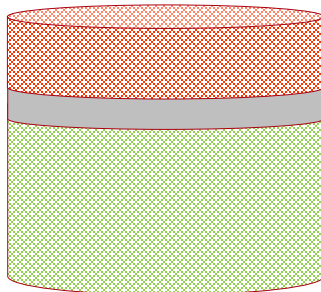
☹️ Delamination

Insufficient lifetime for practical applicability of the technology

Materials and operation of a typical SOC

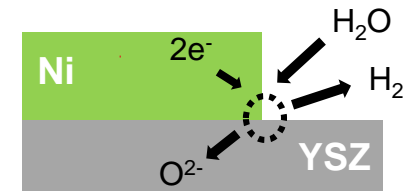
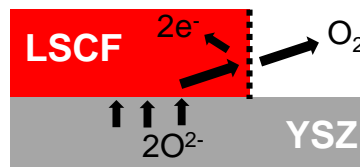
O₂ electrode
Electrolyte

H₂ electrode



- LSCF: Lanthanum Strontium Cobalt Ferrite
- YSZ: Ytria stabilized Zirconia
- Ni-YSZ: ceramic-metallic composite

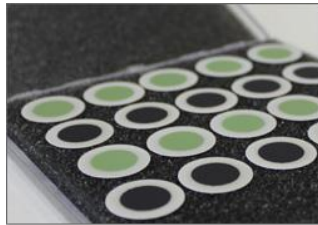
Reactive mechanisms illustrated in SOEC mode at both electrodes:



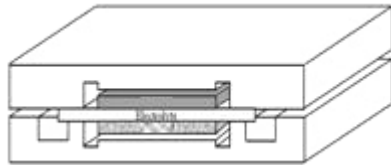
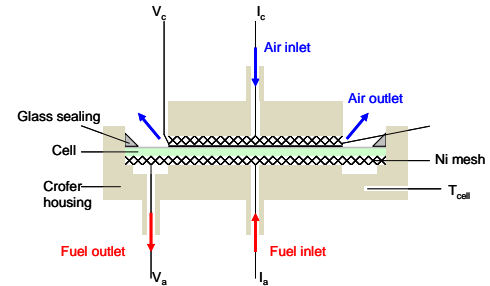
Microstructure evolution detrimental on cell performances

METHODOLOGY

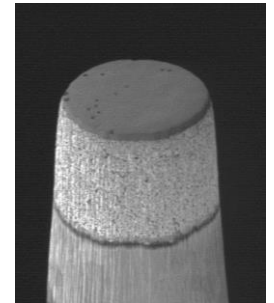
A coupled experimental and modelling approach



Electrochemical test

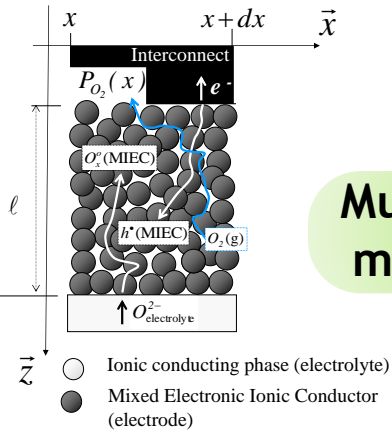
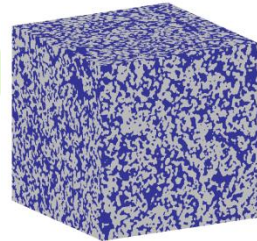


Forecast
Modelling of
SOC



Multi-scale
modelling

Microstructural
characterization

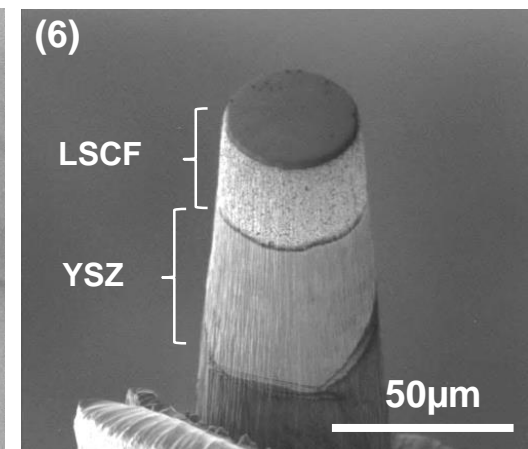
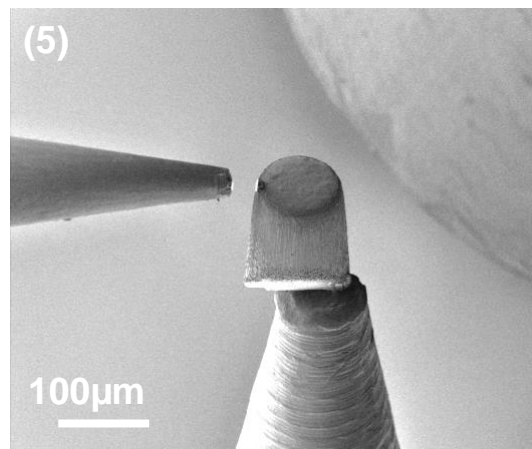
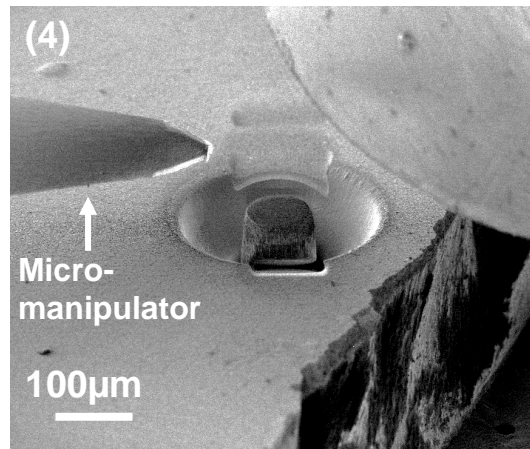
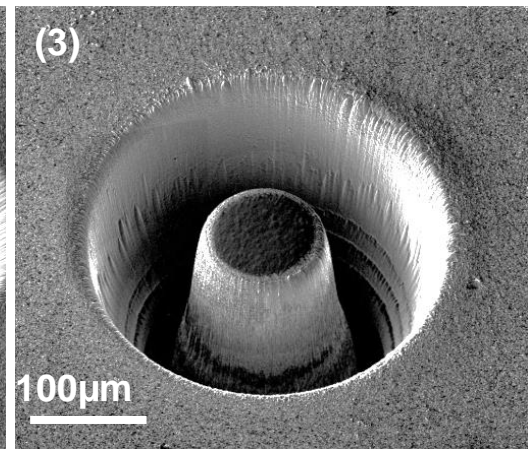
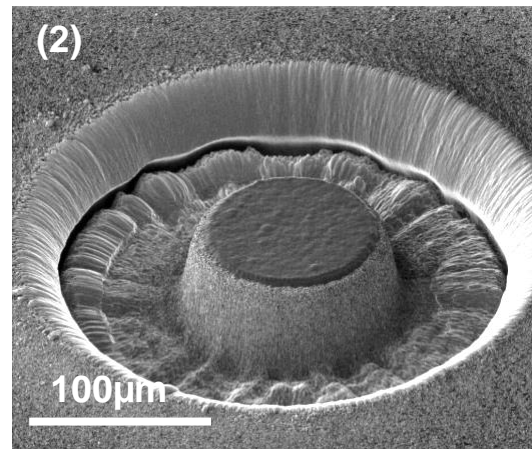
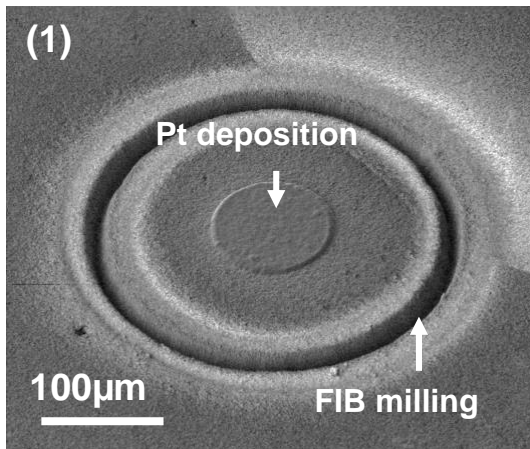


Performance ↔ Microstructure ↔ Degradation

SAMPLE PREPARATION

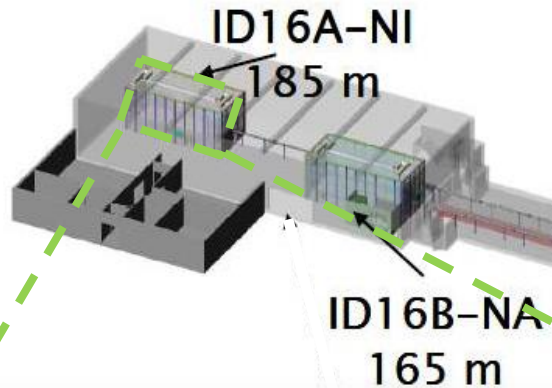
Specific process with Xe Plasma-FIB

- Faster than conventional Ga FIB
- Sample size and localization easily chosen
- Axisymmetric geometry well adapted to tomography



MICROSTRUCTURAL CHARACTERIZATION

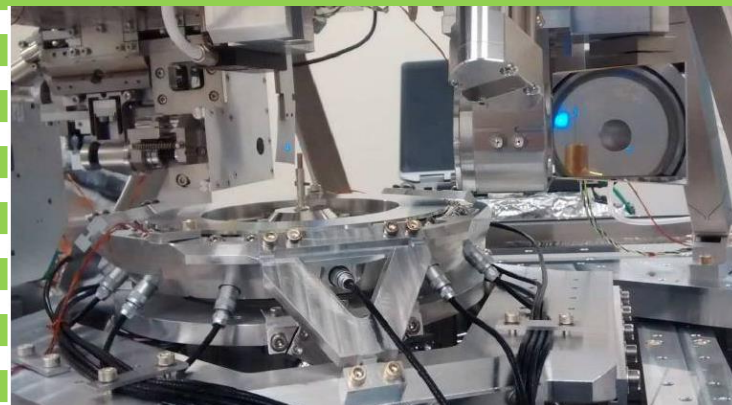
The Nano-Imaging ID16A beamline before EBS



Optics Hutch
34 m

In-vacuum + Cryo
Flux up to $1.4 \cdot 10^{12}$ ph/s at $DE/E = 1\%$
 $E = 17$ keV or 33.6 keV

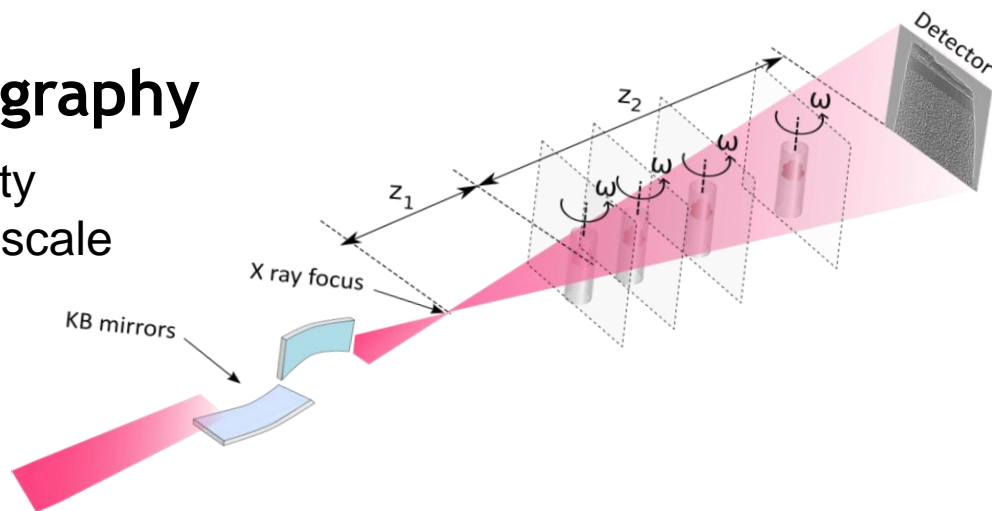
Focused beam: 12-50 nm



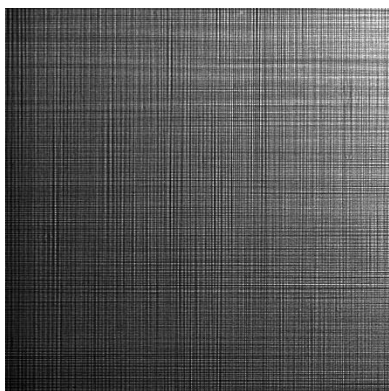
MICROSTRUCTURAL CHARACTERIZATION

Magnified holotomography

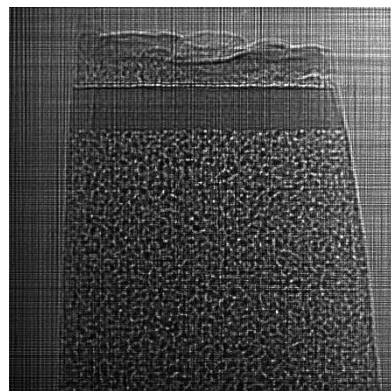
- High electron density sensitivity
- Zoom-in effect, ideal for multi-scale approaches
- Large field of view



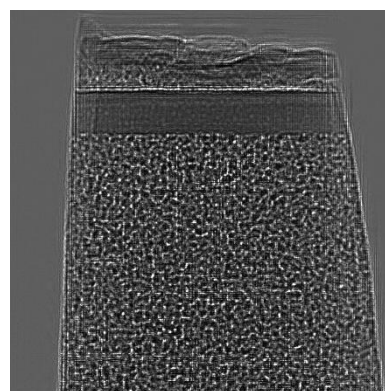
The empty beam correction



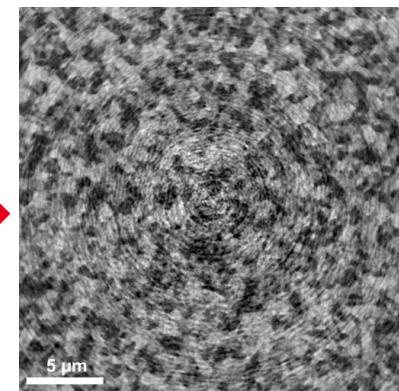
I_{empty}



I_{mixed}



$$\frac{I_{mixed}}{I_{empty}} \approx I_{object}$$



Reconstructed slice
Hydrogen electrode
25nm voxel size

Empty beam correction is non-valid

MICROSTRUCTURAL CHARACTERIZATION

A new acquisition process

Simple model assuming a weak defocusing distance:

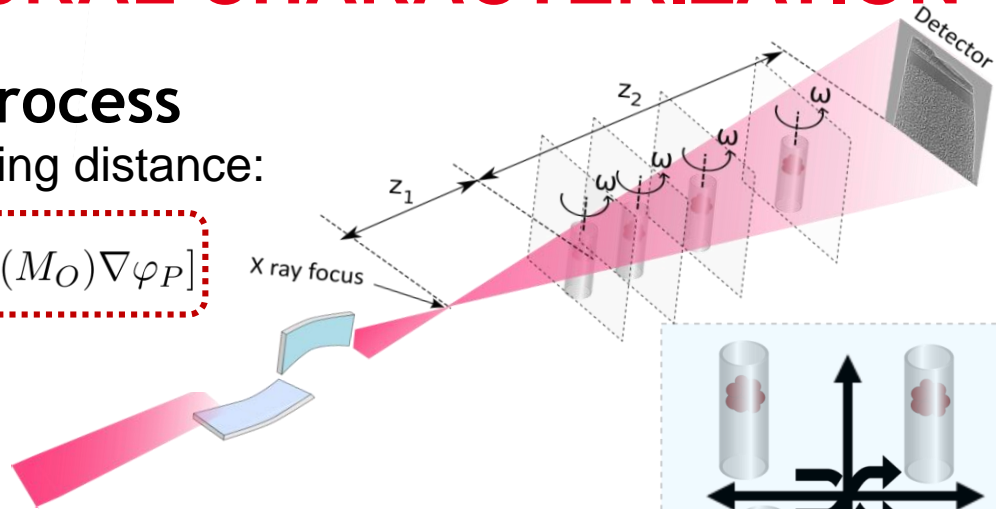
$$\frac{I_{\text{mixed}}}{I_{\text{empty}}} \simeq I_{\text{obj}} - \frac{\lambda z}{\pi} M_O^2 [\nabla \ln(M_P) \nabla \varphi_O + \nabla \ln(M_O) \nabla \varphi_P]$$

“good”
term

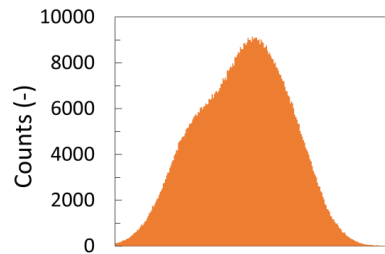
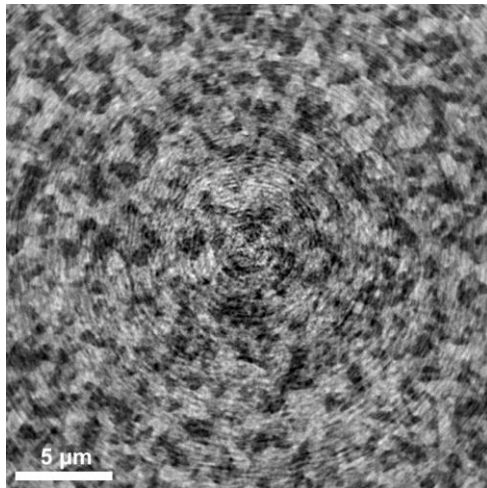
“parasitic” term

Object: $O = M_O \times e^{i\varphi_O}$

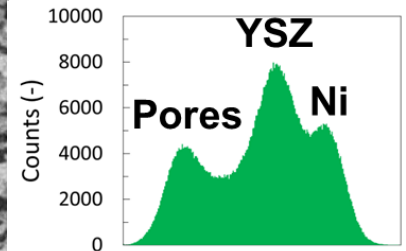
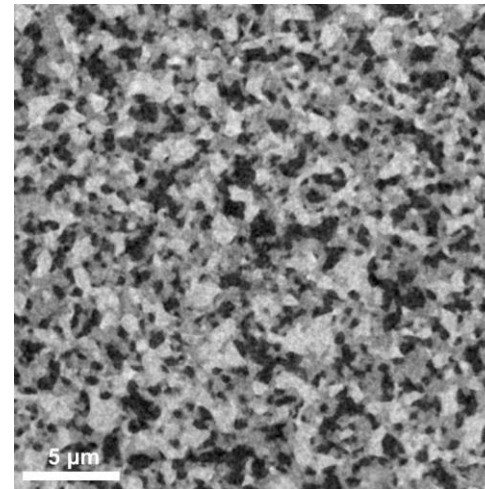
Probe: $P = M_P \times e^{i\varphi_P}$



Random sample displacement smears out the artefacts



Without random



With random

MICROSTRUCTURAL CHARACTERIZATION

A new acquisition process

Simple model assuming a weak defocusing distance:

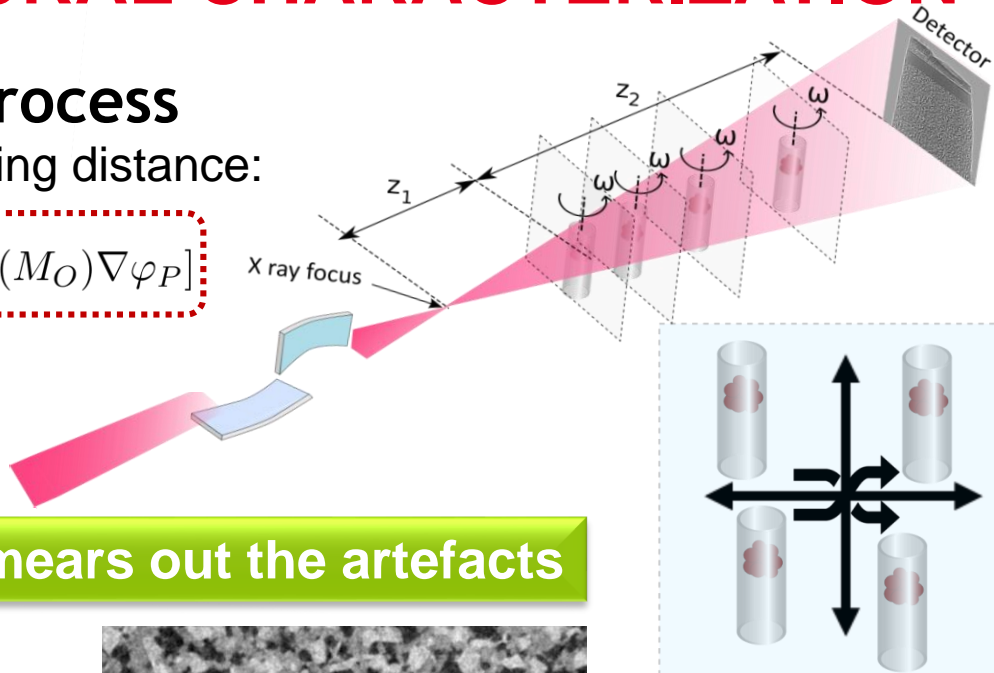
$$\frac{I_{\text{mixed}}}{I_{\text{empty}}} \simeq I_{\text{obj}} - \frac{\lambda z}{\pi} M_O^2 [\nabla \ln(M_P) \nabla \varphi_O + \nabla \ln(M_O) \nabla \varphi_P]$$

“good”
term

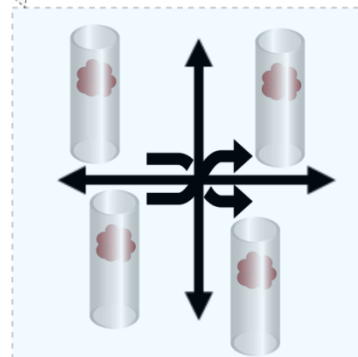
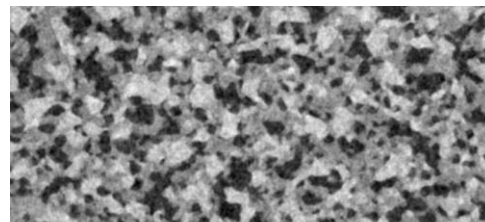
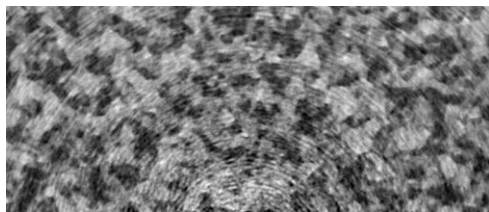
“parasitic” term

Object: $O = M_O \times e^{i\varphi_O}$

Probe: $P = M_P \times e^{i\varphi_P}$



Random sample displacement smears out the artefacts



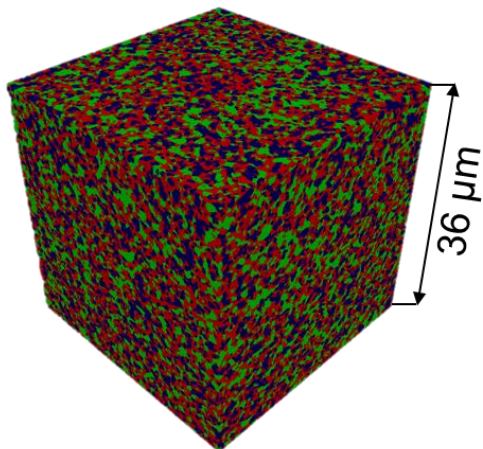
Properties	Pores	YSZ	Ni
Percolated volume fraction (-)	0.280 ± 0.014	0.436 ± 0.003	0.262 ± 0.013
Mean particle diameter (μm)	0.96 ± 0.06	0.60 ± 0.00	1.01 ± 0.03
Specific surface area (μm ⁻¹)*	2.48 ± 0.07	3.62 ± 0.03	2.09 ± 0.09
Tortuosity factor (-)	8.46	2.27	7.45
Active Triple phase boundary length density (μm ⁻²)		4.75 ± 0.08	

Microstructural properties of the Ni-YSZ electrode

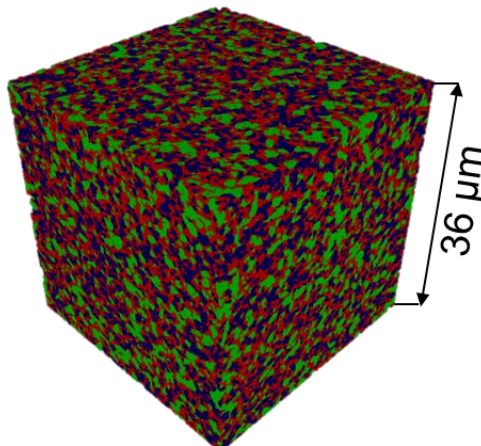
MICROSTRUCTURE ANALYSES

Nickel agglomeration in H₂ electrode

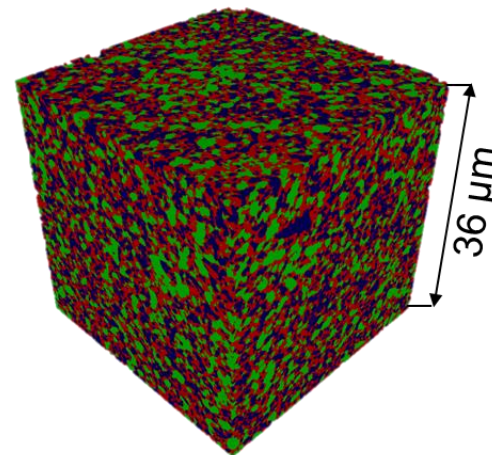
Reference



Aged 1000h



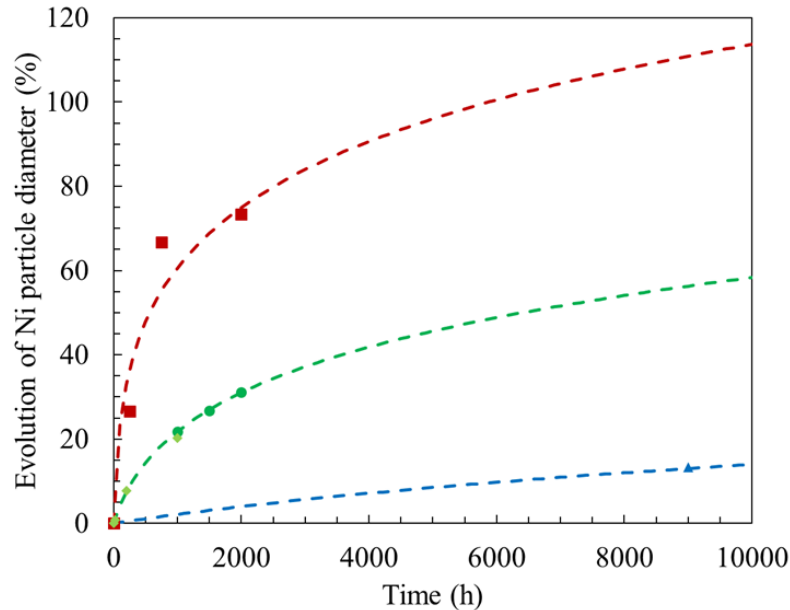
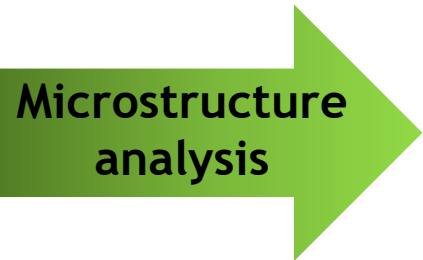
Aged 9000h



■ Ni
 ■ YSZ
 ■ Pores

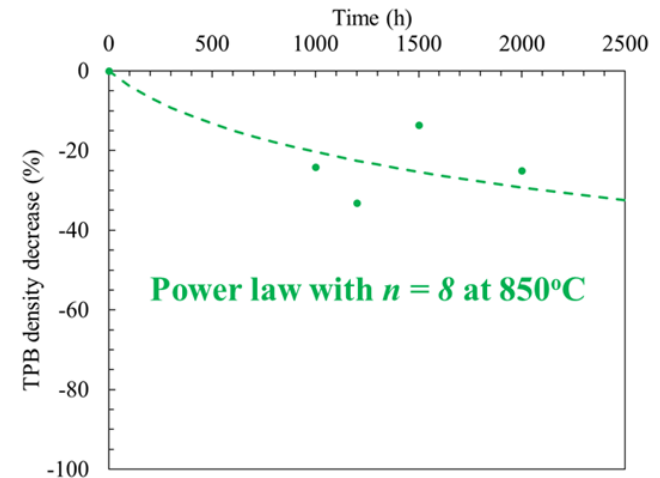
MICROSTRUCTURE ANALYSES

Nickel agglomeration in H₂ electrode



- Data from this work at 850°C
- ▲ Data from this work at 750°C
- ◆ Data from (1) at 850°C
- Data from (2) at 1000°C

(1) P. Tanasini et al. , Fuel Cells, 9 (2009) 740
 (2) S.P. Jiang , J. Mat. Sc., 38 (2003) 3775



- Significant Ni agglomeration
- Significant decrease of the electrochemically active sites
- Inhibiting effect of the YSZ backbone on Ni agglomeration

Contribution of Ni agglomeration on performance losses can be extracted from these analyses (about 25-30%)

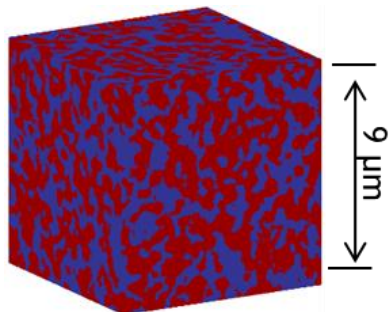
MICROSTRUCTURE ANALYSES

Synthetic microstructure modelling

- Experimental approach based on the manufacturing and characterization of many samples is time consuming
→ The modeling of synthetic microstructure can be an alternative method

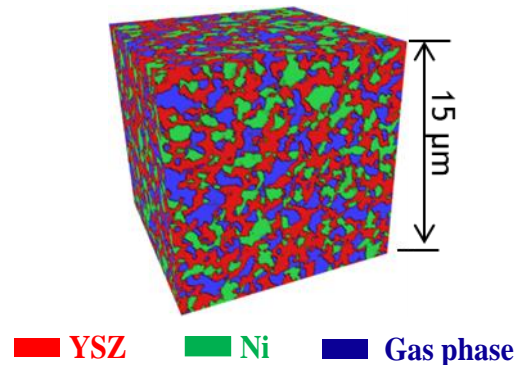
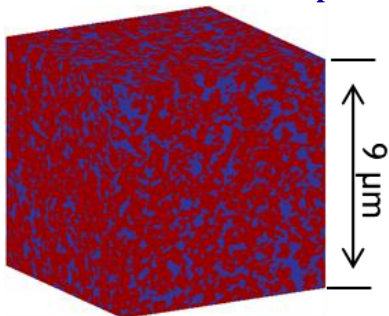
Real electrode microstructures are required for model validation

Cell-1

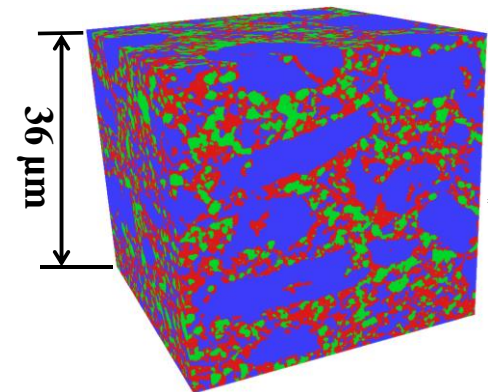
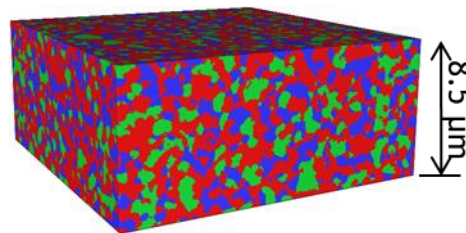


■ LSCF ■ Gas phase

Cell-2

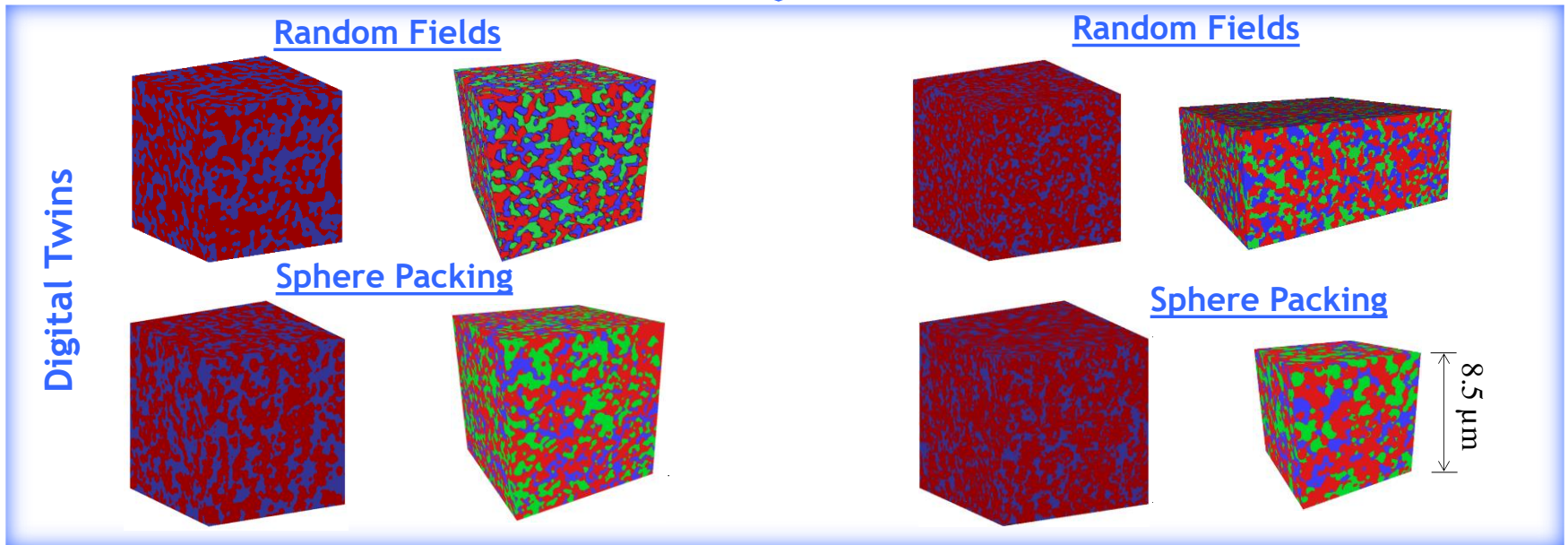
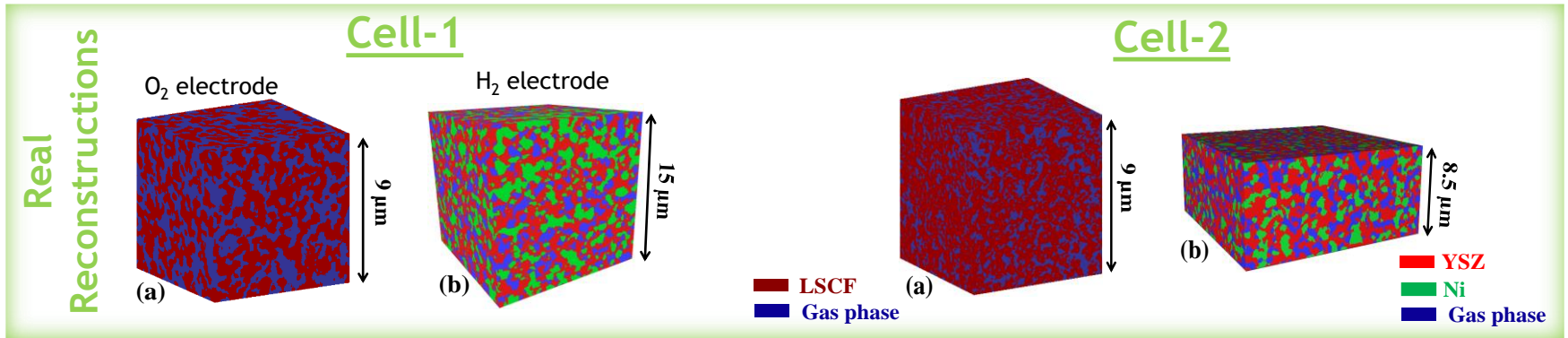


■ YSZ ■ Ni ■ Gas phase



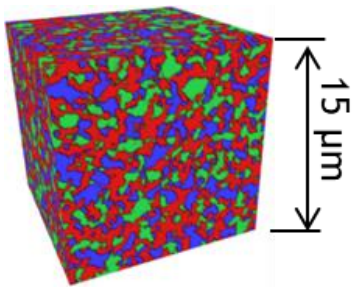
Large range of real 3D electrode microstructure

MICROSTRUCTURE ANALYSES



MICROSTRUCTURE ANALYSES

Illustration on a Ni-YSZ electrode



	YSZ Phase						Active TPBL density (μm^{-2})
	Volume fraction (%)	Phase diameter (μm)	Specific Surface Area (μm^{-1})	Geometrical tortuosity factor (-)	Constrictivity (-)	M-factor (-)	
Random field	~0%	+3%	-1%	~0%	~0%	~0%	-1%
Real reconstruction	44.08	0.28	3.68	1.43	0.13	0.189	4.78
Sphere packing	~0%	~0%	-4%	-1%	-3%	+2%	+4%

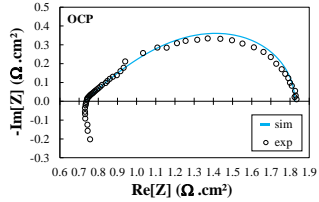
	Gas phase						Ni phase					
	Volume fraction (%)	Phase diameter (μm)	Specific surface area (μm^{-1})	Geometrical tortuosity factor (-)	Constrictivity (-)	M-factor (-)	Volume fraction (%)	Phase diameter (μm)	Specific surface area (μm^{-1})	Geometrical tortuosity factor (-)	Constrictivity (-)	M-factor (-)
Random field	~0%	~0%	-1%	-3%	+22%	+21%	~0%	+3%	+1%	-3%	+22%	+22%
Real reconstruction	28.04	0.28	2.67	1.67	0.09	0.03	27.88	0.33	2.30	1.75	0.08	0.041
Sphere packing	~0%	~0%	-2%	-3%	+16%	+17%	~0%	~0%	-2%	-6%	+18%	+21%

The mismatch does not exceed few percents (except for constrictivity)

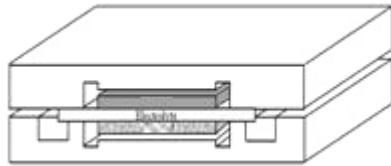
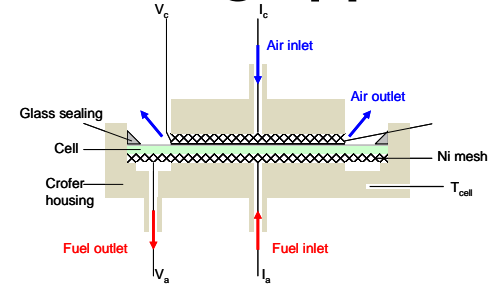
Similar results with the other electrodes

OVERVIEW

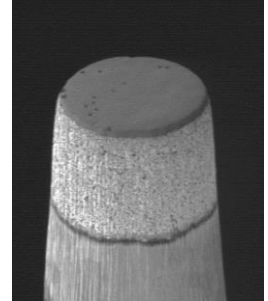
Integrated experimental and modelling approach



Electrochemical test

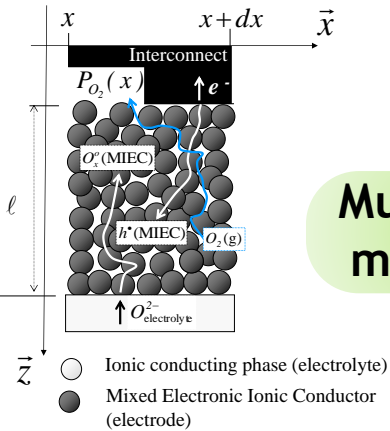
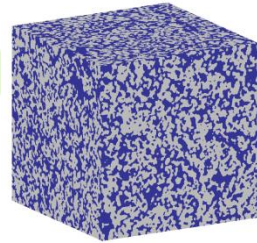


« Multi-scale »
&
« Multi-physic »
modelling



Multi-scale
modelling

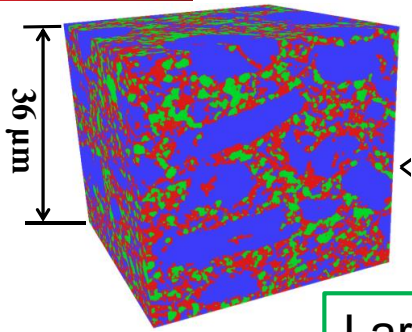
Microstructural
characterization



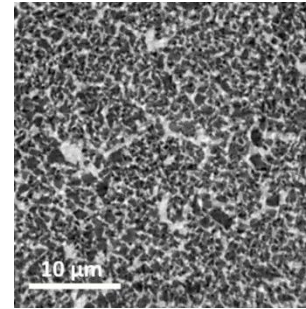
- Ionic conducting phase (electrolyte)
- Mixed Electronic Ionic Conductor (electrode)

Validated numerical tools to investigate SOC

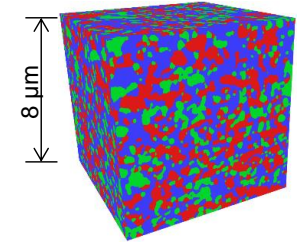
NEW OPPORTUNITIES WITH EBS



Larger field of view



Higher contrast



■ GDC ■ LSCF ■ pores

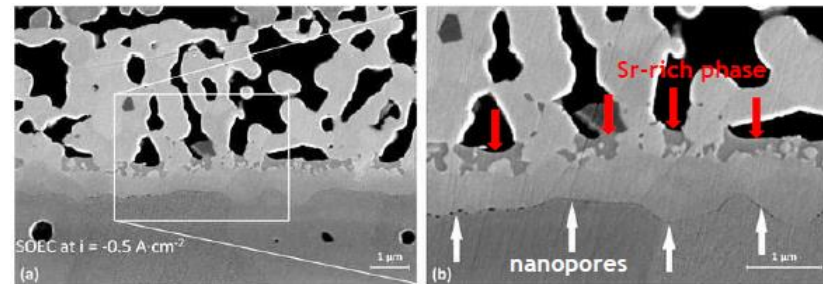
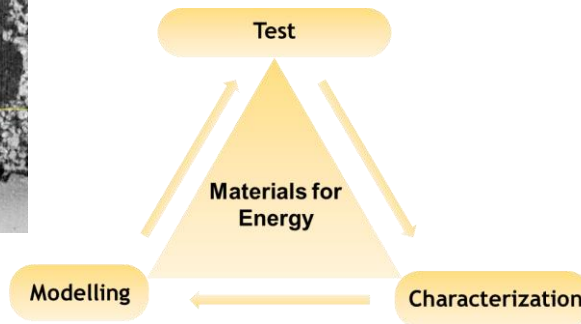
E. Effori et al., Fuel Cells (2019)

Higher spatial resolution



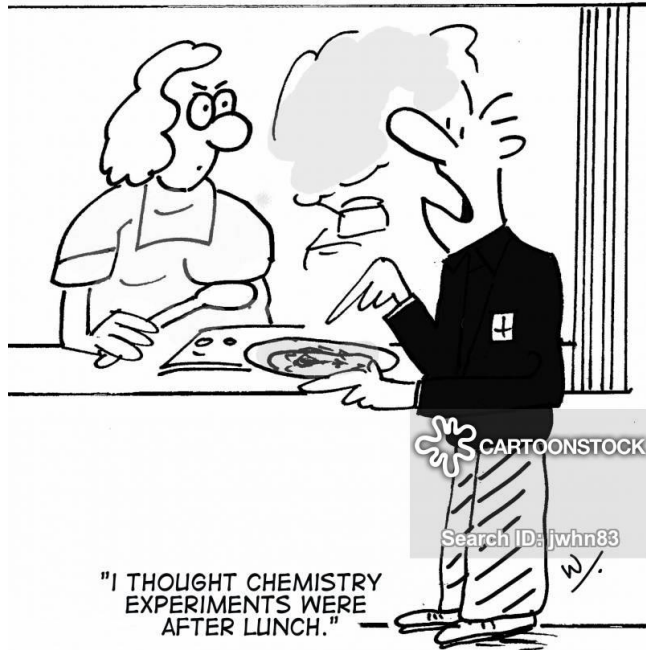
Coupled characterizations

Extend method to materials for energy



J. Laurencin et al., Electrochimica Acta (2017), 459-476

SCHOOL CANTEEN



"I THOUGHT CHEMISTRY
EXPERIMENTS WERE
AFTER LUNCH."

Thank you for your attention

Commissariat à l'énergie atomique et aux énergies alternatives
17 rue des Martyrs | 38054 Grenoble Cedex
www-liten.cea.fr

Établissement public à caractère industriel et commercial | RCS Paris B 775 685 019

Workshop on Coherence at ESRF-EBS | 12-09-2019 | Maxime HUBERT